EJO European Journal of Ophthalmology

Original research article

European Journal of Ophthalmology
1–8

DOI: 10.1177/1120672119852026
journals.sagepub.com/home/ejo
SAGE

Effect of the variability in implantation depth of intracorneal ring segments using the femtosecond laser technology in corneal ectasia

Cristina Peris-Martínez[1,2], Cristina Dualde-Beltrán[3], Ester Fernández-López[1], Maria José Roig-Revert[1], Mikhail Hernández-Díaz[1,2] and David P Piñero[4]

Abstract

Purpose: To analyze the impact of the depth of implantation of intracorneal ring segments on morphological, biomechanical, and clinical outcomes in ectatic corneas.

Methods: This prospective longitudinal study enrolled 40 eyes of 29 patients (age 20–51 years) with corneal ectasia that underwent intracorneal ring segments implantation (KeraRing, Mediphacos). Changes in visual acuity, refraction, corneal tomography, and corneal biomechanics (Ocular Response Analyzer, Reichert) were evaluated during a 6 month follow-up. Likewise, changes in ring segment implantation depth measured by optical coherence tomography (Visante OCT, Carl Zeiss Meditec) were also evaluated.

Results: Mean relative depth of implantation was 71.6 ± 5.8%, 71.5 ± 6.5%, and 71.9 ± 6.3% at 1, 3, and 6 months after surgery, respectively ($p = 0.827$). The difference between the real relative depth of implantation and the theoretical attempted value of 70% was not statistically significant ($p = 0.072$). Differences in spherical equivalent during the follow-up changed significantly depending on the level of relative depth of implantation ($p = 0.036$), with an increase of 0.114 D per each 1% increase in relative depth of implantation. Likewise, a decrease of –0.194 D in the steepest keratometric reading was found per each decrease of 1% in relative depth of implantation ($p = 0.026$). Changes in corneal thickness ($p = 0.092$) and biomechanics ($p = 0.080$) were not related to relative depth of implantation.

Conclusion: The effect on visual acuity and refraction of intracorneal ring segments when implanted in corneal ectasia is less clinically relevant when the implantation is done at a very deep plane. The variability of the depth of intracorneal ring segments implantation when using femtosecond laser technology is minimal and with no clinically significant effect on clinical outcomes.

Keywords

Corneal ectasia, intracorneal ring segment, keraring, femtosecond, keratoconus

Date received: 22 October 2018; accepted: 9 April 2019

[1]Cornea and External Diseases Unit, FISABIO-Oftalmología Médica (FOM), Valencia, Spain
[2]Clínica Oftalmológica Aviñó&Peris, Valencia, Spain
[3]Hospital Universitario Doctor Peset, Valencia, Spain
[4]Department of Optics, Pharmacology and Anatomy, University of Alicante, Alicante, Spain

Corresponding authors:
Cristina Peris-Martínez, Cornea and External Diseases Unit, FISABIO-Oftalmología Médica (FOM), Av. Pío Baroja, 12, 46035 València, Spain.
Email: crisperis@ono.com

David P Piñero, Department of Optics, Pharmacology and Anatomy, University of Alicante, Crta San Vicente del Raspeig s/n 03016, San Vicente del Raspeig, Alicante, Spain.
Email: david.pinyero@ua.es

Introduction

The implantation of intracorneal ring segments (ICRS) in corneal ectasia has been demonstrated to be an effective therapeutic option for improving visual acuity and reducing corneal aberrations and irregularity.[1] However, in spite of the improvements in the nomograms of implantation of ICRS,[1–5] some unexpected results are still present in clinical practice, requiring adjustments and even the explantation of the ring segment.[6,7] One of the reasons for this is that the mechanism of these implants in relation to the level of mechanical weakening of the ectatic cornea is not still completely understood, although some simulation models of the potential effect of ICRS have been developed.[8–10] Besides changes in anterior corneal surface shape,[11] the implantation of ICRS has shown to induce significant changes in the geometry of the posterior corneal surface that are in most of cases unpredictable.[12–14] Furthermore, it has been demonstrated that the correlation between the visual outcomes after ICRS implantation and tomographic measurements is poor.[15]

Several factors have been defined as critical for predicting the effect generated by ICRS, such as ring thickness and diameter.[16] There is a nearly linear relationship between the degree of central corneal flattening induced and ring thickness.[17,18] Indeed, the selection of the ring segment to implant in one specific case is based on the definition of the ring thickness, besides the arc length.[19] For the selection of these parameters, different criteria or nomograms have been defined according to the type of ring segment that are based on considering different clinical variables, such as refraction, corneal asphericity or corneal topography pattern.[19] However, the depth of implantation of the ring segment is not considered in nomograms of ICRS implantation in spite of being the parameter that affects the corneal optics the most according to simulations used in silico models.[8] Currently, the use of the femtosecond laser technology allows the creation of tunnels for ICRS insertion at a predictable depth,[20] although long-term changes in this depth can occur possibly due to biomechanical or structural modifications and the scrubbing habit of these patients that can modify the position of the rings.[21,22] The aim of the current study was to analyze and characterize the impact of the depth of implantation of ICRS on morphological, biomechanical, and clinical outcomes obtained in ectatic corneas.

Methods

Patients

This was a prospective longitudinal study enrolling a total of 40 eyes of 29 patients with corneal ectasia (keratoconus, pellucid marginal degeneration, and post-LASIK ectasia) that underwent ICRS implantation. All eyes were operated on at the Cornea and Anterior Segment Unit of Fisabio Oftalmología Médica (FOM) and at the Aviñó & Peris Eye Clinic, both in Valencia (Spain), with the implantation of KeraRing® segments (Mediphacos, Belo Horizonte, Brazil), which has a triangular section profile.[19] The diagnosis of corneal ectasia was based on the following criteria: the presence of an asymmetric bowtie pattern in corneal topography and at least one of the following clinical signs on slit-lamp, such as stromal thinning, conical protrusion of the cornea at the apex, Fleischer ring, Vogt striae or anterior stromal scar.[23] This study was approved by the FOM's Ethics Committee and was performed in accordance with the ethical standards laid down in the 1964 Declaration of Helsinki. Written informed consent was obtained from all subjects, being free to withdraw participation at any time without reason.

Inclusion criteria for the study were patients of at least 18 years, presence of corneal ectasia according to the criteria previously defined, transparent central cornea, contact lens intolerance, and a mesopic pupil size of 5.5 mm or lower. Exclusion criteria were ocular media opacity, previous ocular surgery except corneal laser refractive surgery, underlying corneal dystrophy or trauma, active systemic or ocular diseases, altered eyelid anatomy and function, and pregnancy. No contact lens fitting was prescribed in any case during the follow-up of this study.

Examination protocol

A preoperative examination was performed in all cases. This examination included anamnesis, uncorrected distance visual acuity (UDVA) and corrected distance visual acuity (CDVA), manifest refraction, slit-lamp examination, corneal topographic and pachymetric analysis (Pentacam HR, Oculus OptikgeräteGmbH, Wetzlar, Germany), corneal biomechanical analysis (Ocular Response Analyzer (ORA) version 2.04, Reichert-DePew, NY, Inc.), and funduscopy. Postoperatively, follow-up visits were performed at 1 day, 1, 3, and 6 months after surgery. The following tests were performed at 1, 3 and 6 months after surgery: slit-lamp examination, corneal topography and aberrometry, measurement of UDVA and CDVA, manifest refraction, corneal biomechanical analysis with the ORA system, and cornea analysis by means of anterior segment optical coherence tomography (OCT) (Visante OCT, Carl Zeiss Meditec, Jena Germany). It should be remarked that all biomechanical measurements during the follow-up were obtained in the morning from 9:00 to 12:00 a.m. to reduce the effects of diurnal corneal variations.[24] Concerning OCT images, once they were obtained, the depth of implantation of ICRS was calculated as follows considering the relationship between distances represented in Figure 1:

Implantation depth (segment DE) = Corneal thickness at the area of implantation (segment DF) – Depth of the base of segment (segment EF)

Besides the depth of implantation of ICRS, the relative implantation depth was also calculated as follows (Figure 1):

Relative implantation depth = 100 x (Corneal thickness at the area of implantation DF – Depth of the base of segment EF / Corneal thickness at the area of implantation DF)

In case of a cornea with two ring segments implanted, the mean relative depth of both segments was calculated.

Surgical technique

All surgical interventions were performed by the same expert surgeon (C.P.) using topical anesthesia. In all cases, incisions were placed on the steepest meridian according to the topographic map. The 60 kHz IntraLase® femtosecond laser system (IntraLase, IntraLase Corp.) was used to create the corneal tunnels for the insertion of ring segments. Initially, the center of the pupil was marked on the slit-lamp followed by the application of the vacuum suction ring. The disposable glass lens of the laser system was then applanated to the cornea to fixate the eye, allowing to maintain a precise distance from the laser head to the focal point. Then, a continuous circular stromal tunnel was created at approximately 70% of corneal depth. Once this procedure was finished, the ring segment was inserted, and the corneal incision was hydrated with intrastromal cefuroxime. In all cases, KeraRing® segments were implanted, which are made of polymethyl methacrylate (PMMA) and have a triangular transverse section as well as a variable thickness from 150 to 350 μm. The selection of the number, arc length, and thickness of the segments implanted in each case was made according to the nomogram defined by the manufacturer.[1]

Topical tobramycin-dexamethasone eyedrops (TobraDex®, Alcon Labs) were prescribed to be used postoperatively every 6 h for 1 week. Likewise, a topical lubricant containing polyethylene glycol 0.4% and propylene glycol 0.3% (Systane®) was prescribed to be applied every 6 h for 1 month.

Statistical analysis

Data analysis was performed with a commercially available software package (SPSS for Mac, Version 22.0; IBM Corporation, Armonk, NY, USA). First, a descriptive analysis of all variables was performed that included calculation of mean, standard deviation (SD), median, minimum and maximum for continuous variables, and calculation of absolute and relative frequencies for categorical variables. After this, normality of data samples was evaluated by means of the Kolmogorov–Smirnov test. In the subgroup of eyes with two ring segments implanted, the Wilcoxon test was used to contrast the positional measurements of both segments. A repeated analysis of variance measure

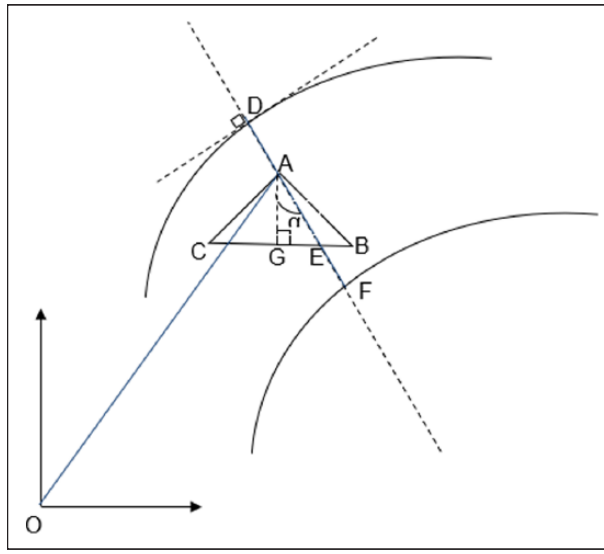

Figure 1. Diagram showing the relationships between different anatomical distances within the cornea. The depth of implantation of each ring segment (segment DE) was calculated as the subtraction of the depth of the base of the segment (segment EF) from the total corneal thickness at the area of implantation (segment DF).

(ANOVA) was used to evaluate if the ring segment depth remained stable during the follow-up. The Student t-test for paired measurements was used to contrast if the mean relative implantation depth of each ring segment was consistent with the theoretical value of 70%. Finally, the change analysis of the different clinical variables evaluated according to the implantation was performed by means of generalized estimating equation (GEE) models considering the follow-up time point and the eye as intra-subject variables, and the depth as continuous time-dependent predictor. Thus, the model considered that the corneal structure where the ring segment was implanted was a dynamic environment, with a position of the ring segment that can change over time. Likewise, the correlations between eyes of the same patient are considered. The matrix of correlations selected was interchangeable, independent or not structured according to the criteria of goodness of adjustment of independence of the model. For all statistical tests, a p-value of less than 0.05 was considered as statistically significant.

The statistical power achieved with the GEE model was based on a random model of linear multiple regression. A relationship between ring segment implantation depth and any clinical parameter with at least R^2 of 0.35 should be detected with a statistical power of 75.5% for $N=29$ ($\alpha=0.05$, 2 tails and $k=3$ predictors).

For the analysis of refractive changes, all spherocylindrical refractions obtained were converted to vectorial notation using the power vector method described by Thibos and Horner.[25]

Table 1. Summary of the main outcomes obtained in the study.

Mean (SD) Median (Range)	Preoperative	1 month post operation	3 months post operation	6 months post operation
LogMAR UDVA	0.82 (0.35) 0.82 (0.30 to 1.30)	0.52 (0.36) 0.52 (0.00 to 1.30)	0.50 (0.37) 0.40 (0.05 to 1.30)	0.49 (0.31) 0.40 (0.05 to 1.30)
Manifest sphere (D)	−1.54 (4.13) –1.38 (–16.00 to 5.00)	−1.23 (3.00) –1.00 (–12.00 to 5.00)	−1.09 (2.62) –1.00 (–9.00 to 4.00)	−0.94 (2.48) –0.75 (–6.00 to 4.00)
Manifest cylinder (D)	−3.73 (1.89) –3.88 (–8.00 to 0.00)	−2.48 (1.56) –2.25 (–8.00 to 0.00)	−2.67 (1.58) –3.00 (–8.00 to 0.00)	−2.73 (1.20) –3.00 (–5.00 to 0.00)
Manifest SE (D)	−3.41 (4.44) –2.88 (–19.00 to 3.63)	−2.47 (3.31) –2.00 (–14.00 to 3.00)	−2.42 (3.00) –2.00 (–11.50 to 3.00)	−2.29 (2.66) –2.00 (–8.00 to 1.75)
Manifest J_0 (D)	0.46 (1.22) 0.01 (–2.10 to 2.99)	0.20 (1.08) 0.00 (–1.50 to 3.61)	0.07 (1.12) 0.00 (–1.49 to 3.61)	−0.01 (1.15) 0.03 (–2.00 to 1.99)
Manifest J_{45} (D)	−0.07 (1.66) –0.06 (–2.98 to 3.99)	−0.03 (0.99) 0.00 (–2.00 to 2.28)	0.01 (1.10) 0.00 (–1.96 to 2.70)	−0.03 (0.97) 0.15 (–2.00 to 2.21)
Manifest B (D)	4.68 (3.69) 3.80 (0.00 to 19.24)	3.22 (2.96) 2.24 (0.00 to 14.14)	3.24 (2.57) 2.83 (0.00 to 11.77)	3.09 (2.23) 2.83 (0.71 to 8.25)
LogMAR CDVA	0.29 (0.19) 0.30 (0.00 to 0.82)	0.23 (0.27) 0.15 (0.00 to 1.30)	0.21 (0.24) 0.17 (0.00 to 1.30)	0.22 (0.22) 0.15 (0.00 to 1.00)
CCT (μm)	473.1 52.4) 471.5 (375 to 581)	475.1 (56.8) 484.0 (365 to 591)	486.5 (60.0) 493.0 (360 to 592)	478.8 (56.8) 480.0 (370 to 580)
MCT (μm)	454.7 (52.0) 456.5 (350 to 566)	468.5 (67.4) 469.5 (354 to 591)	474.6 (61.5) 481.0 (337 to 591)	467.7 (59.2) 474.5 (341 to 569)
K1 (D)	45.64 (5.00) 45.40 (33.30 to 55.90)	44.94 (4.50) 44.65 (36.50 to 55.50)	44.40 (4.58) 43.90 (35.30 to 55.80)	44.73 (4.52) 44.55 (35.00 to 52.70)
K2 (D)	51.74 (6.07) 50.10 (41.90 to 65.70)	49.50 (5.74) 48.15 (38.90 to 61.00)	48.34 (5.49) 47.70 (39.30 to 61.00)	48.93 (5.36) 47.75 (38.10 to 59.30)
CH (mmHg)	8.20 (1.68) 8.30 (5.20 to 13.80)	8.24 (2.10) 8.20 (3.90 to 14.30)	8.50 (1.89) 8.10 (4.20 to 14.10)	9.06 (2.71) 8.60 (5.50 to 13.60)
CRF (mmHg)	7.37 (2.06) 6.60 (4.90 to 12.90)	7.81 (2.14) 7.70 (3.70 to 12.30)	7.17 (1.91) 7.00 (3.40 to 11.40)	7.73 (2.93) 7.10 (3.80 to 12.4)

SD: standard deviation; UDVA: uncorrected distance visual acuity; SE: spherical equivalent; J_0 and J_{45}: astigmatic power vector components; B: overall blurring strength; CDVA: corrected distance visual acuity; CCT: central corneal thickness; MCT: minimum corneal thickness; K1:eratometric corneal power in the flattest meridian; K2:eratometric corneal power in the steepest meridian; CH: corneal hysteresis; CRF: corneal resistance factor.

Results

The sample included a total of 40 eyes of 29 patients (69.0% males and 31.0% females) with a mean age of 33.2 years (SD = 8.6, median = 33, range = 20–51 years). A total of 22 right (55.0%) and 18 left (45.0%) eyes were included. Concerning the type of corneal ectasia, the distribution of cases in our series was as follows: 11 eyes (27.5%) with keratoconus grade II (Amsler-Krumeich grading system), 22 eyes (55.0%) with keratoconus grade III, 4 eyes (10.0%) with pellucid marginal degeneration, and 3 eyes (7.5%) with post-LASIK ectasia. Table 1 summarizes the changes in visual, refractive, topographic, and tomographic data during the follow-up.

Ring segment implantation depth

Mean absolute ring implantation depth was 0.456 ± 0.055 mm, 0.448 ± 0.062 mm, and 0.448 ± 0.052 mm at 1, 3, and 6 months after surgery, respectively. Mean relative depth of implantation was 71.6% (SD = 5.8, median = 71.8, range = 55.7%–85.1%), 71.5% (SD = 6.5, median = 71.0, range = 55.7%–85.9%), and 71.9% (SD = 6.3, median = 71.3, range = 57.4%–87.0%) at 1, 3, and 6 months after surgery, respectively. Changes in this parameter during the follow-up were not statistically significant (p = 0.827). Mean relative depth of implantation during all this follow-up was 71.7% (SD = 5.7; median = 71.9; range = 57.4%–84.5%). The difference between the real relative depth of implantation and the theoretical attempted value of 70% was not statistically significant (p = 0.072, confidence interval (CI) 95% = 69.8, 73.5%).

Effect of ring segment implantation depth on visual and refractive outcomes

The GEE model established that changes in UDVA over time were statistically significant (p = 0.004), with an improvement of –0.036 logMAR units per month. However, the relative depth of implantation did not have an important effect on these changes (p = 0.774). Similarly, changes in CDVA over time were also statistically significant (p = 0.001) and independent from the relative depth of implantation (p = 0.447), with an improvement of –0.015 logMAR units per month.

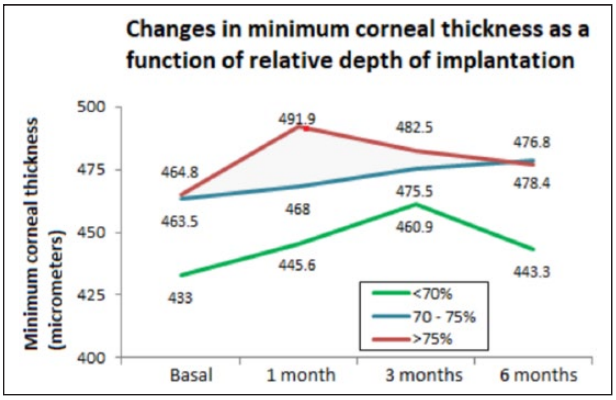

Figure 2. Changes in minimum corneal pachymetry during the follow-up as a function of the relative depth of implantation of ring segments (<70% green line, 70%–75% blue line, and >75% red line).

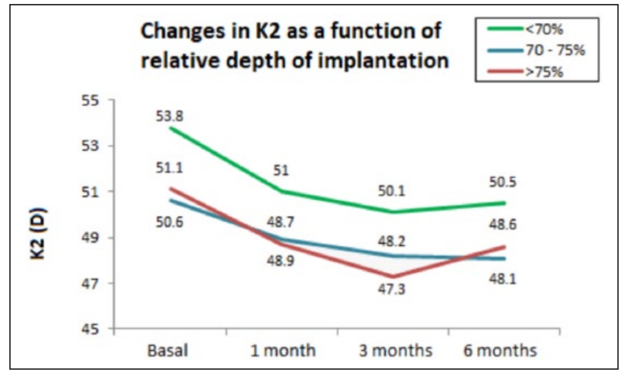

Figure 3. Changes in steepest keratometric reading (K2) during the follow-up as a function of the relative depth of implantation of ring segments (<70% green line, 70%–75% blue line, and >75% red line).

Concerning the spherical equivalent, differences in changes during the follow-up were detected depending on the level of relative implantation depth (p = 0.036), with an increase of 0.114 D per each 1% increase in relative implantation depth. In contrast, there was no statistically significant association between changes in astigmatic power vector components of manifest refraction and relative depth of implantation (J_0 p = 0.670, J_{45} p = 0.432). Changes over time during the follow-up in spherical equivalent (p = 0.193), J_0 (p = 0.070), and J_{45} (p = 0.769) did not reach statistical significance. Finally, the GEE detected a very pronounced effect of time on B, but it did not reach statistical significance (p = 0.060), with a decrease of –0.18 D in B per month. Likewise, some level of dependency was found between B and relative depth of implantation (p = 0.077), with a trend to lower values of B in eyes with deeper implants.

Effect of ring segment implantation depth on pachymetry

The GEE model confirms the presence of a progressive increase of minimum corneal pachymetry with time during the follow-up (p = 0.013) (Figure 2), with an increasing rate of 1.68 µm per month. No statistically significant trend toward higher pachymetric values was found in eyes with deeper implants (p = 0.092).

Effect of ring segment implantation depth on topography

Significant changes were found in the flattest keratometric reading (K1) over time during the follow-up (p < 0.001), with a keratometric decrease of –0.089 D per month. Similarly, significant changes with time were found in the steepest keratometric reading (K2), with a decrease of –0.398 D per month. Whereas the relative depth of implantation did not have a significant effect on changes in K1 (p = 0.230), it was significantly associated with changes in K2 (Figure 3) (p = 0.026). Specifically, there was a decrease of –0.194 D in K2 per each decrease of 1% in relative depth of implantation.

Effect of ring segment implantation depth on ORA biomechanical parameters

Changes over time during the follow-up in corneal hysteresis (CH) (p = 0.066) and corneal resistance factor (CRF) (p = 0.716) did not reach statistical significance. Likewise, no significant associations were found between the relative depth of implantation of ring segment and the parameters CH (p = 0.080) and CRF (p = 0.202).

Discussion

In the current study, we have confirmed first that the depth of implantation planned was not significantly different than that really achieved using the femtosecond technology for the creation of corneal tunnels. This is consistent with the results of previous studies showing a high level of accuracy in the lamellar dissection achieved with the femtosecond laser.[26–28] Monteiro et al.[26] found in a multicenter comparative study that ICRS implantation assisted by a femtosecond laser was a more precise procedure in terms of dissection depth when compared with the manual dissection technique. Naftali and Jabaly-Habib[29] found that the depth of implantation of ICRS measured by OCT was less than expected when the mechanical technique was used for ring segment implantation. A similar result was also reported by Lai et al.[30] and by Barbara et al.[31] using Intacs ring segments in keratoconus as well as by Gorgun et al.[32] using KeraRing segments. The more controlled mode of generating the corneal tunnels with femtosecond laser technology has been shown to be related to significantly better clinical results compared to the classical mechanical dissection in different types of corneal ectasia.[11,33,34] Likewise, the less superficial implantation of ICRS achieved with femtosecond laser technology than with the mechanical procedure has been shown to be in relation with a lower incidence of ring segment position-related complications.[19] Only Kouassi et al.[35] found in a prospective comparative study that both mechanical and femtosecond laser-assisted Intacs implantations showed a more superficial ring segment placement than predicted, with no statistically significant difference between techniques. Differences in the sample evaluated and in the clinical and surgical protocols followed in this study and in the study of Monteiro et al.,[26] and by our research group in the current series may account for this discrepancy.

In our sample, the depth of implantation did not change significantly during the follow-up, suggesting that the level of stability of the implant within the corneal structure is ensured. It should be considered that OCT technology has been shown to be a valid tool to evaluate longitudinal changes occurring in ICRS position over time after their implantation.[36] However, longer follow-ups are needed to provide consistent conclusions about the positional stability of ring segments within the corneal structure. Indeed, Shahhoseini et al.[20] demonstrated in a retrospective study that ring segments were placed at a shallower depth than originally intended at 26 months after their implantation. More studies concerning this issue are still needed to obtain consistent conclusions.

The variability in the depth of implantation of ICRS in our series did not have an important effect on visual outcomes. Therefore, this factor has a minimal impact on vision when the femtosecond laser technology is used for creating the tunnels where the ring segments are implanted. This is consistent with the study of Hashemi et al.[37] showing the greatest UDVA and CDVA improvements with ICRS in post-LASIK ectasia with implantation depths between 60%–79%, a range covering our range of variability. In spite of this relative absence of dependence between visual outcomes and the variability of the depth of implantation of ring segments, a statistically significant trend to an increase in spherical equivalent of 0.114 D per each change of 1% in relative implantation depth was found. Therefore, less degree of myopia correction was achieved with the deepest implants. This is consistent with the findings of Hashemi et al.[37] that demonstrated that ICRS implantation depths greater than 80% of stromal thickness have minimal or null effect on visual and topographic status. In this line, we found that there was a decrease of –0.194 D in the K2 per each decrease of 1% in relative depth of implantation. All these outcomes are consistent with biomechanical simulations reported showing that the stromal depth insertion was the parameter that seemed to affect the corneal optics the most and consequently refraction, whereas the horizontal distance of ring insertion and the diameter of the ring's cross-section were less important.[8]

Finally, we analyzed the association of relative depth of implantation with pachymetric and corneal biomechanical changes. This association was found to be not statistically significant and therefore changes in these parameters with ICRS implantation were non-significantly influenced by the relative depth of implantation, considering the range evaluated in this study. As a limitation, it should be mentioned that in most of our eyes the relative depth of implantation was 70% or above, with a limited sample of cases with more anterior implants. According to simulations, ICRS inserted deeper would prevent keratoconus in the posterior stroma from increasing (relaxation of posterior surface), but will promote its growing if they are located in the anterior surface (increment of stress).[8] Indeed, relevant rates of ring segment extrusion have been reported in eyes with more anterior implantation of segments.[19] Likewise, Lai et al.[30] found in a prospective observational case series that shallower placement of ICRS may result in more complications, such as epithelial-stromal breakdown and extrusion, because of the greater anterior stromal tensile strain. Another limitation is our corneal biomechanical analysis that was based on the use of the ORA system that provides two biomechanical parameters, CH and CRF, whose relationship with the standard mechanical properties used to define the behavior of any structure is not completely understood.[38] Future studies using more accurate technologies to evaluate the mechanical response of the cornea to the peripheral insertion of ICRS should be conducted.

In conclusion, the implantation of ICRS in corneal ectasia generates a corneal flattening mainly in the steepest meridian leading to a refractive change. This effect is dependent on the depth of implantation of the ring segments, with less clinically relevant effect on visual acuity and refraction for very posterior implantations. There is some level of variability in the relative depth of implantation when femtosecond laser technology is used for such purpose, but this variability has a very limited impact on the clinical outcomes achieved. Future studies should be conducted to evaluate the impact of depth of implantation on the aberrometric control achieved with the ring segments.

Declaration of conflicting interests

The author(s) declared no potential conflicts of interest with respect to the research, authorship, and/or publication of this article.

Disclosure

The authors have no proprietary or commercial interest in the medical devices that are involved in this article.

Funding

The author(s) disclosed receipt of the following financial support for the research, authorship, and/or publication of this article: The author David P Piñero has been supported by the Ministry of Economy, Industry and Competitiveness of Spain within the program Ramón y Cajal, RYC-2016-20471.

References

1. Pinero DP, Alio JL, Teus MA, et al. Modeling the intracorneal ring segment effect in keratoconus using refractive, keratometric, and corneal aberrometric data. *Invest Ophthalmol Vis Sci* 2010; 51(11): 5583–5591.
2. Lisa C, Fernández-Vega Cueto L, Poo-López A, et al. Long-term follow-up of intrastromal corneal ring segments (210-degree arc length) in central keratoconus with high corneal asphericity. *Cornea* 2017; 36: 1325–1330.
3. Fernández-Vega Cueto L, Lisa C, Madrid-Costa D, et al. Long-term follow-up of intrastromal corneal ring segments in paracentral keratoconus with coincident corneal keratometric, comatic, and refractive axes: stability of the procedure. *J Ophthalmol* 2017; 2017: 4058026.
4. Israel M, Yousif MO, Osman NA, et al. Keratoconus correction using a new model of intrastromal corneal ring segments. *J Cataract Refract Surg* 2016; 42(3): 444–454.
5. Fernandez-Vega Cueto L, Lisa C, Poo-Lopez A, et al. Intrastromal corneal ring segment implantation in 409 paracentral keratoconic eyes. *Cornea* 2016; 35(11): 1421–1426.
6. Monteiro T, Mendes JF, Faria-Correia F, et al. Adjustment of intrastromal corneal ring segments after unsuccessful implantation in keratoconic eyes. *Cornea* 2018; 37(2): 182–188.
7. Chan K and Hersh PS. Removal and repositioning of intracorneal ring segments: improving corneal topography and clinical outcomes in keratoconus and ectasia. *Cornea* 2017; 36: 244–248.
8. Flecha-Lescun J, Calvo B, Zurita J, et al. Template-based methodology for the simulation of intracorneal segment ring implantation in human corneas. *Biomech Model Mechanobiol* 2018; 17: 923–938.
9. Daxer A. Biomechanics of corneal ring implants. *Cornea* 2015; 34: 1493–1498.
10. Lago MA, Rupérez MJ, Monserrat C, et al. Patient-specific simulation of the intrastromal ring segment implantation in corneas with keratoconus. *J Mech Behav Biomed Mater* 2015; 51: 260–268.
11. Piñero DP, Alio JL, El Kady B, et al. Refractive and aberrometric outcomes of intracorneal ring segments for keratoconus: mechanical versus femtosecond-assisted procedures. *Ophthalmology* 2009; 116: 1675–1687.
12. Muftuoglu O, Aydin R and Kilic Muftuoglu I. Persistence of the cone on the posterior corneal surface affecting corneal aberration changes after intracorneal ring segment implantation in patients With keratoconus. *Cornea* 2018; 37: 347–353.
13. Torquetti L, Arce C, Merayo-Lloves J, et al. Evaluation of anterior and posterior surfaces of the cornea using a dual Scheimpflug analyzer in keratoconus patients implanted with intrastromal corneal ring segments. *Int J Ophthalmol* 2016; 9: 1283–1288.
14. Söğütlü E, Piñero DP, Kubaloglu A, et al. Elevation changes of central posterior corneal surface after intracorneal ring segment implantation in keratoconus. *Cornea* 2012; 31: 387–395.
15. Lyra JM, Lyra D, Ribeiro G, et al. Tomographic findings after implantation of Ferrara intrastromal corneal ring segments in keratoconus. *J Refract Surg* 2017; 33(2): 110–115.
16. Patel S, Marshall J and Fitzke FW III. Model for deriving the optical performance of the myopic eye corrected with an intracorneal ring. *J Refract Surg* 1995; 11(4): 248–252.
17. Burris TE, Baker PC, Ayer CT, et al. Flattening of central corneal curvature with intrastromal corneal rings of increasing thickness: an eye-bank eye study. *J Cataract Refract Surg* 1993; 19: 182–187.
18. Nosé W, Neves RA, Schanzlin DJ, et al. Intrastromal corneal ring—one-year results of first implants in humans: a preliminary non-functional eye study. *Refract Corneal Surg* 1993; 9: 452–458.
19. Pinero DP and Alio JL. Intracorneal ring segments in ectatic corneal disease—a review. *Clin Exp Ophthalmol* 2010; 38(2): 154–167.
20. Shahhoseini S, Hashemi H and Asgari S. Intracorneal ring segment depth in keratoconus patients: a long-term follow-up study. *Int Ophthalmol* 2017; 38: 1379–1383.
21. Vega-Estrada A, Alió JL and Plaza-Puche AB. Keratoconus progression after intrastromal corneal ring segment implantation in young patients: five-year follow-up. *J Cataract Refract Surg* 2015; 41: 1145–1152.
22. Piñero DP, Alio JL, Barraquer RI, et al. Corneal biomechanical changes after intracorneal ring segment implantation in keratoconus. *Cornea* 2012; 31: 491–499.
23. Pinero DP, Nieto JC and Lopez-Miguel A. Characterization of corneal structure in keratoconus. *J Cataract Refract Surg* 2012; 38(12): 2167–2183.
24. Gonzalez-Meijome JM, Queiros A, Jorge J, et al. Intraoffice variability of corneal biomechanical parameters and intraocular pressure (IOP). *Optom Vis Sci* 2008; 85(6): 457–462.
25. Thibos LN and Horner D. Power vector analysis of the optical outcomes of refractive surgery. *J Cataract Refract Surg* 2001; 27: 80–85.
26. Monteiro T, Alfonso JF, Franqueira N Jr, et al. Predictability of tunnel depth for intrastromal corneal ring segments implantation between manual and femtosecond laser techniques. *J Refract Surg* 2018; 34(3): 188–194.
27. Ozgurhan EB, Agca A, Bozkurt E, et al. Accuracy and precision of cap thickness in small incision lenticule extraction. *Clin Ophthalmol* 2013; 7: 923–926.
28. Khoramnia R, Salgado JP, Lohmann CP, et al. Precision, morphology, and histology of corneal flap cuts using a 200-kHz femtosecond laser. *Eur J Ophthalmol* 2012; 22(2): 161–167.
29. Naftali M and Jabaly-Habib H. Depth of intrastromal corneal ring segments by OCT. *Eur J Ophthalmol* 2013; 23(2): 171–176.
30. Lai MM, Tang M, Andrade EM, et al. Optical coherence tomography to assess intrastromal corneal ring segment depth in keratoconic eyes. *J Cataract Refract Surg* 2006; 32(11): 1860–1865.
31. Barbara R, Barbara A and Naftali M. Depth evaluation of intended vs actual Intacs intrastromal ring segments using optical coherence tomography. *Eye (Lond)* 2016; 30(1): 102–110.
32. Gorgun E, Kucumen RB, Yenerel NM, et al. Assessment of intrastromal corneal ring segment position with anterior segment optical coherence tomography. *Ophthalmic Surg Lasers Imaging* 2012; 43(3): 214–221.

33. Pinero DP, Alio JL, Uceda-Montanes A, et al. Intracorneal ring segment implantation in corneas with post-laser in situ keratomileusis keratectasia. *Ophthalmology* 2009; 116(9): 1665–1674.
34. Pinero DP, Alio JL, Morbelli H, et al. Refractive and corneal aberrometric changes after intracorneal ring implantation in corneas with pellucid marginal degeneration. *Ophthalmology* 2009; 116(9): 1656–1664.
35. Kouassi FX, Buestel C, Raman B, et al. Comparison of the depth predictability of intra corneal ring segment implantation by mechanical versus femtosecond laser-assisted techniques using optical coherence tomography (OCT Visante). *J Fr Ophtalmol* 2012; 35(2): 94–99.
36. Perez-Merino P, Ortiz S, Alejandre N, et al. Quantitative OCT-based longitudinal evaluation of intracorneal ring segment implantation in keratoconus. *Invest Ophthalmol Vis Sci* 2013; 54(9): 6040–6051.
37. Hashemi H, Yazdani-Abyaneh A, Beheshtnejad A, et al. Efficacy of Intacs intrastromal corneal ring segment relative to depth of insertion evaluated with anterior segment optical coherence tomography. *Middle East Afr J Ophthalmol* 2013; 20(3): 234–238.
38. Pinero DP and Alcon N. In vivo characterization of corneal biomechanics. *J Cataract Refract Surg* 2014; 40(6): 870–887.